Ultrasound in Med. & Biol., Vol. 27, No. 5, pp. 683–693, 2001

0301-5629/01/$–see front matter

ELSEVIER

PII: S0301-5629(01)00345-3

● *Original Contribution*

THE MECHANISMS OF STONE FRAGMENTATION IN ESWL

WOLFGANG EISENMENGER
Physikalisches Institut der Universität Stuttgart, Stuttgart, Germany

(*Received* 15 *September* 2000; *in final form* 22 *January* 2001)

Abstract—Currently, several mechanisms of kidney stone fragmentation in extracorporal shockwave lithotripsy (ESWL) are under discussion. As a new mechanism, the circumferential quasistatic compression or "squeezing" by evanescent waves in the stone has been introduced. In fragmentation experiments with self-focussing electromagnetic shock-wave generators with focal diameters comparable to or larger than the stone diameter, we observed first cleavage surfaces either parallel or perpendicular to the wave propagation direction. This is in agreement with the expectation of the "squeezing" mechanism. Because, for positive pulse pressures below 35 MPa and stones with radii of 15 mm or smaller, cleavage into only two fragments was observed, we developed a quantitative model of binary fragmentation by "quasistatic squeezing." This model predicts the ratio of the number of pulses for the fragmentation to 2-mm size and of the number of pulses required for the first cleavage into two parts. This "fragmentation-ratio" depends linearly alone on the stone radius and on the final size of the fragments. The experimental results for spherical artificial stones of 5 mm, 12 mm and 15 mm diameter at a pulse pressure of 11 MPa are in good agreement with the theoretical prediction. Thus, binary fragmentation by quasistatic squeezing in ESWL as a new efficient fragmentation mechanism is also quantitatively verified. (E-mail: w.eisenmenger@physik.uni-stuttgart.de) © 2001 World Federation for Ultrasound in Medicine & Biology.

Key Words: **ESWL, Shock-wave lithotripsy, Fatigue, Coalescence of microcracks, Evanescent waves, Binary fragmentation, Squeezing, Cohesive zone model, Cavitation, Brittle materials, Artificial stones, Fragmentation ratio.**

INTRODUCTION

Extracorporal shockwave lithotripsy (ESWL) has been extremely successful in treating human kidney stones for the past 20 years. The history of this unique development is documented in review articles (Coleman and Saunders 1993; Delius 1994, 2000) and textbooks (Chaussy et al. 1997; Eisenberger et al. 1991). Increasing perfection in three lithotripter generations has led to systems of high fragmentation efficiency and minimal side effects. Despite this success, there is still only limited agreement on the relevant fragmentation mechanisms. Also, the question of how to further optimise the physical parameters of the pressure or shock waves with respect to fragmentation results and avoidance of side effects remains open (Delius 2000; Lokhandwalla and Sturtevant 2000; Sturtevant and Lokhandwalla 1998).

The present contribution discusses a new mechanism (Eisenmenger 1998) of stone destruction in ESWL that possibly may help to find an answer to the open questions.

Address correspondence to: Prof. W. Eisenmenger, Univ. Stuttgart, 1 Physikalisches Institut, Pfaffenwaldring 57, D-70550 Stuttgart, Germany. E-mail: w.eisenmenger@physik.uni-stuttgart.de

ESWL

Stone fragmentation mechanisms. Because fragmentation needs tensile stress or strain, the pressure wave in ESWL pulses consisting of a positive and a negative part can act in different ways. The positive part (Lokhandwalla and Sturtevant 2000) can only result in significant tensile stress if it is narrower in space extension in the stone than the dimension of the stone itself; thus, creating pressure gradients, shear stress and, finally, tensile stress and strain. This is especially the case if the focus diameter is small compared to the stone diameter, resulting first in more crater-like (Fig. 1) fragmentation erosion (Granz and Köhler 1992; Vakil et al. 1991), as observed with most sharply focusing ESWL systems.

Less sharply focused pulses or plane pressure waves of duration shorter than the traveling time in the stone are transmitted into the stone and reflected at the sound soft stone-water posterior (rear) interface with pressure inversion; thus, splitting off stone material by the tensile

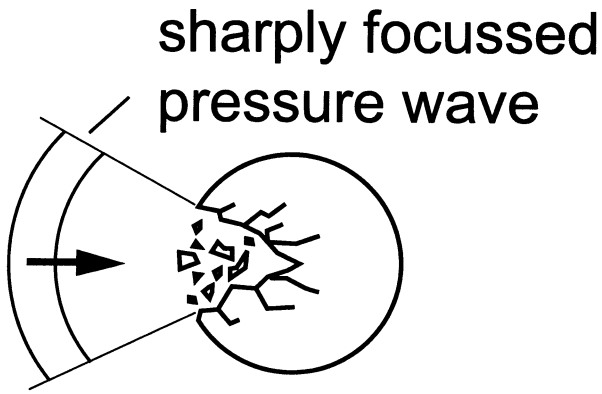

Fig. 1. Schematic crater-like fragmentation erosion in ESWL with a sharp focus of 2 to 6 mm −6-dB focal width and larger stone diameter.

stress in the reflected wave (Delius 1994), known as the Hopkinson effect. A similar situation appears for wedge reflection at the posterior part of the stone, as described in (Lokhandwalla and Sturtevant 2000). Also, the focusing of the reflected tensile waves in the stone has been analysed (Dahake and Gracewski 1997a,b) together with computer simulations.

The negative part of the pressure wave, instead, acts directly (Lokhandwalla and Sturtevant 2000) on the stone, generating almost homogeneous tensile stress with no confinement in space and time required.

In addition to the direct strain action on the stone, the negative pressure waves cause cavitation in the water surrounding the stone and, also, within the water in the microcracks (Sass et al. 1991) and cleavage interfaces of the stone. Cavitation erosion is especially observed at the anterior and posterior side of artificial stones *in vitro* (Granz and Köhler 1992; Vakil et al. 1991). Delius (1997) observed that the application of moderate static pressures suppressed the ESWL fragmentation of gallstones and reduced the fragmentation of kidney stones significantly. This indicated a strong contribution of fragmentation by cavitation in the fragmentation process.

Recently, it has been shown (Xi and Zhong 2000) that stone fragmentation is significantly enhanced by a second shock wave applied during the collapse of cavitation bubbles generated by a preceding first shock wave.

Stone cleavage. Fragmentation of gallstones and artificial stones *in vitro* under the condition of focus diameter comparable to or larger than the stone diameter resulted after a finite number of pulses in stone cleavage (Sass et al. 1991), mostly into two parts. Holtum (1993) found that 60% of gallstones were cleaved in planes parallel to the wave propagation direction. Other authors report (Sass et al. 1991) cleavage in planes perpendicular to the wave propagation direction. Delius and Gambihler (1991) mentioned cleavage parallel to the wave propagation direction for small stone diameters. These earlier observations of first cleavage planes either parallel or perpendicular to the wave-propagation direction can be explained by a “squeezing” mechanism (Eisenmenger 1998). A detailed experimental and theoretical study of the mechanism is presented in this article. We first discuss the results of new cleavage experiments on the basis of the squeezing model. We further determine the fragmentation ratio (*i.e.,* the number of shock pulses needed for the first cleavage of spherical artificial stones and the pulse number for fragmentation to 2-mm fragment size). The experimental results are, finally, compared with a simple quantitative model of quasistatic squeezing and binary fragmentation. The mathematical theory will be presented in a separate section.

Experimental methods and materials

The fragmentation studies were performed with self-focusing electromagnetic generators (Brümmer et al. 1992; Eisenmenger 1983, 1988; Staudenraus 1991) with 15 to 18 mm −6-dB focal diameter and a positive peak pressure ranging from 10 MPa to 40 MPa operating from the bottom of a water-filled basin or from the side in horizontal wave-propagation direction. Artificial stones were held between two polyethylene films under slight tension by rubber rings (see Fig. 2). Thus, the conditions in the kidney pelvis were simulated because the stone, as well as the fragments, were kept within the focal range surrounded by the liquid.

For pressure pulse measurements, we used the fiberoptic probe hydrophone (FOPH) (IEC 1998; Staudenraus and Eisenmenger 1993; Wang et al. 1999) to determine all pulse characteristics as positive and negative peak pressures, the corresponding pulse duration, the focal dimensions and other parameters. In this report, we restrict to only a few data (Irmer et al. 2001). A detailed mapping of the shockwave field of a commercial lithotripter was obtained with the FOPH 300 and verified mathematically with high accuracy, using finite element analysis (Steiger and Marlinghaus 1997; Steiger 1998).

As material for the fragmentation measurements, we used artificial stones made from plaster of Paris from different sources (Heimbach et al. 2000). Spherical stones of 15 mm diameter and cylindrical stones of 10 mm by 10 mm where supplied by High Medical Technologies A. G., Switzerland (HMT). Also, 5-mm spherical and cylindrical artificial stones came from HMT. Spherical artificial stones of 12 mm diameter were supplied by Dornier Medical Systems. Static compression and tensile stress tests have been performed in our mechanical workshop, shaping the spherical stones of HMT with 15 mm diameter to cylinders. These static measure-

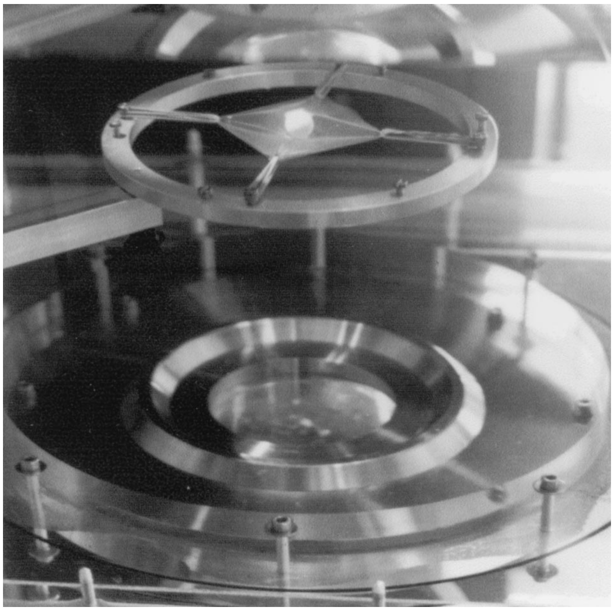

Fig. 2. Shock wave measuring basin of the Biologic Institute of the University of Stuttgart with the self-focusing electromagnetic generator at the bottom and the sample holder above. The stone is placed between the two polyethylene films mounted with four rubber strings to simulate the situation of a stone in the kidney pelvis. The observation and photographic registration of the fragmentation structures is made from above parallel to the direction of the wave-propagation vector (*i.e.*, perpendicular to the picture plane).

ments revealed a surprisingly large difference of the maximum stress and strain of dry and wetted stones from 7.5 MPA to 2.3 MPa for compression and 1.5 MPa to 0.7 MPa for strain, respectively. The HMT stones appear to be about 30% less fragile than the other stones (Heimbach et al. 2000).

As did other authors (Müller 1990), we used a grid of 2-mm mesh size to measure the stone fragmentation efficiency by determining the number of pulses needed until all fragments had passed through. In our arrangement, the artificial stone was placed between two polyethylene foils (see Fig. 3) with a 2-mm mesh size nylon grid underneath. In addition to the fact that the fragmentation rate, (*i.e.*, the reciprocal pulse number for fragmentation to 2 mm size) scaled with the total pulse energy or, more simply, with the square of the pulse peak pressure as reported earlier by several authors (Delius 1994; Dreyer et al. 1998; Irmer 1997; Koch and Grünewald 1989; Müller 1990; Ueberle 1997, 2000), we observed a reproducible relation between the pulse number for the final fragmentation to 2-mm size and the number of pulses for the first cleavage. The results are compared with a simple fragmentation model based on the squeezing mechanism, together with binary fragmentation.

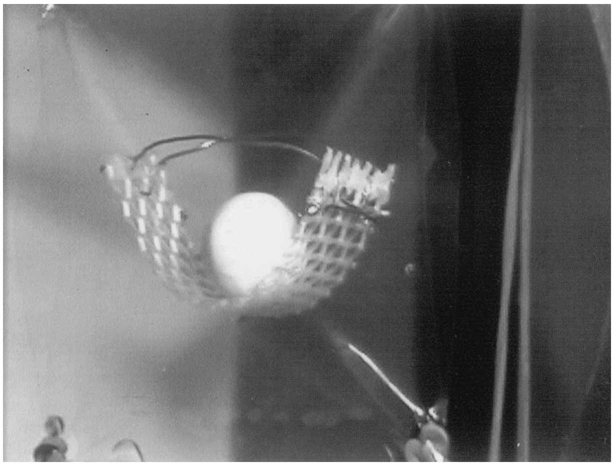

Fig. 3. Artificial stone (HMT) of 15-mm diameter between two polyethylene foils fixed with rubber strings and a 2-mm mesh size nylon grid underneath. For the fragmentation measurements, the pressure pulse now propagates horizontally from left to right.

RESULTS

Cleavage of sperical stones by squeezing

In fragmentation experiments with a self-focusing electromagnetic generator, we observed cleavage in planes parallel to the wave vector (see Fig. 4) with positive pulse-pressure amplitudes of 20 MPa and cleavage in planes perpendicular to the wave vector with lower pressures of 10 MPa. These very reproducible observations of first cleavage planes either parallel or perpendicular to the wave-propagation direction as reported also by other authors (Sass et al. 1991; Holtum 1993; Delius and Gambihler 1991), are in accord with

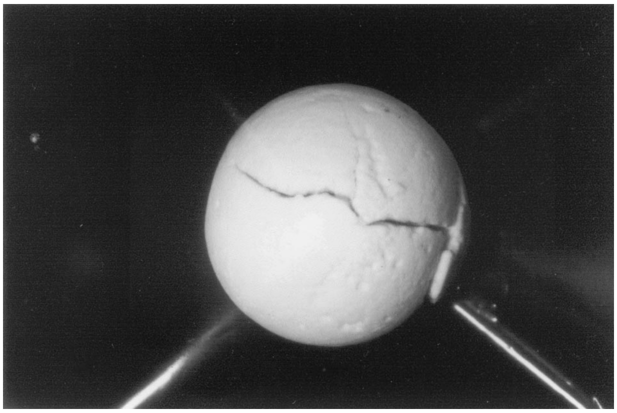

Fig. 4. First cleavage parallel to the wave-propagation direction of a 15-mm diameter HMT artificial stone after 7 shock-wave exposures at 32.5 MPa, pulse duration 1.5 μs and 17 mm -6-dB focal diameter as observed parallel to the shock-wave propagation direction.

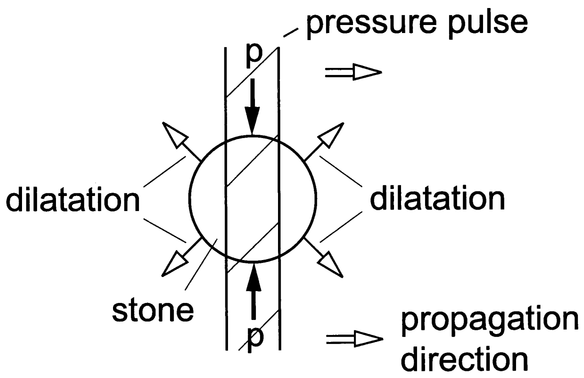

Fig. 5. Circumferential quasistatic ring compression or "squeezing" by the pressure pulse propagating in the surrounding liquid or tissue. The stone dilatation is indicated by open one-line arrows, the wave propagation direction is indicated by open double-line arrows. The lateral pressure exerted by the wave on the stone is indicated by closed arrows.

Fig. 7. Cleavage of an artificial stone (HMT 15 mm) by static squeezing. The stone is inserted into a piece of silicon rubber hose and placed in a hose clamp that has been steadily tightened to exert circumferential pressure.

the squeezing mechanism (Eisenmenger 1998). In this mechanism, the part of the pressure wave traveling outside of the stone surface exerts a circular pressure and causes, inside the stone, a compression zone (see Fig. 5) moving with the sound velocity in water. Because this velocity is below the elastic wave propagation velocities in the stone, the resulting compression zone in the stone is moving quasistatically as an evanescent wave (as the evanescent wave in total reflection). The inhomogeneously pressurised region of 1 to 3 mm width corresponding to the pulse width in water, causes tensile stress in the adjoining nonpressurised areas of the stone, as depicted for an artificial stone of 15 mm diameter in Fig. 6 at the moment of the wave position at the centre plane of the stone. From Fig. 6, it is evident that the maximal dilatation strains are at the stone anterior and posterior surfaces in directions perpendicular to the wave vector whereas, in the centre of the stone, the maximal dilatation strain is parallel to the wave vector.

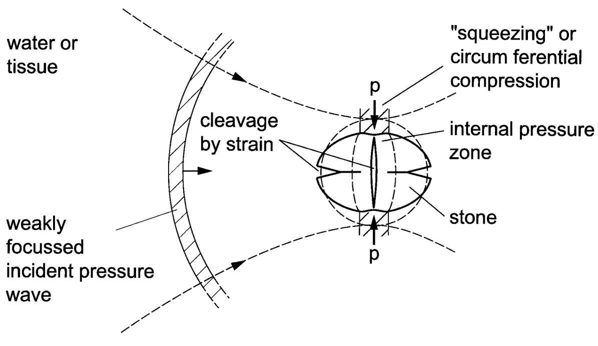

Fig. 6. Cleavage plane orientations by the "squeezing" mechanism. At the anterior and the posterior surfaces, the resulting strain is perpendicular to the wave-propagation direction. In the interior of the stone, the resulting strain is parallel to the wave-propagation direction.

For a static simulation of the squeezing mechanism, we inserted an artificial stone of 15 mm diameter into a 10 mm long piece of silicon rubber hose placed into a hose clamp that was carefully tightened for squeezing the stone. The fragmentation result is shown in Fig. 7, obviously in agreement with Fig. 4.

Thus, the observation of cleavage planes either parallel or perpendicular to the wave propagation direction can be explained by the squeezing mechanism. These two alternatives of first cleavage have been observed in several further examples with stones of different shapes.

Cleavage of cylindrical stones by squeezing

As shown in Fig. 8 cylindrical artificial stones also exhibit a first cleavage parallel to the wave-propagation direction. Additional pulse exposure results in further cleavage parallel to the wave-propagation direction and also in cleavage perpendicular to the wave vector, as observed in Fig. 9. If the cylindrical axis of the artificial stone is parallel to the wave vector, cleavage in a plane perpendicular to the wave vector results in two shorter cylindrical fragments, as shown in Fig. 10.

Multiple first cleavage planes

With larger stones or with higher pressures, the first cleavage of cylindrical stones (Fig. 11) may show several fracture planes parallel and perpendicular to the wave-propagation direction, in agreement with the expectation of the squeezing model. Spherical artificial stones show three first cleavage planes parallel to the wave-propagation direction (Fig. 12) with increased pulse pressure. With further increased pressure pulse amplitude or with

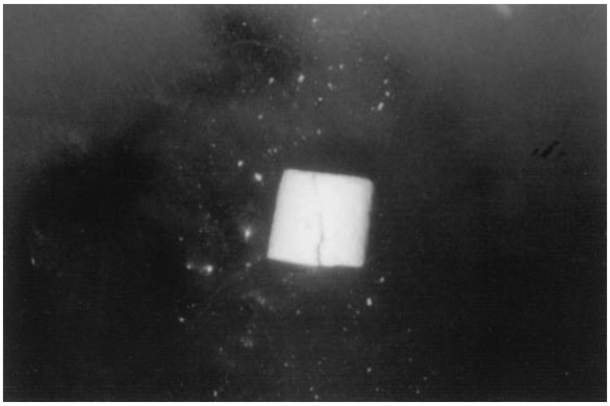

Fig. 8. First cleavage of a cylindrical artificial stone parallel to the wave-propagation direction. The stone (Dornier) dimensions are 5 × 5 mm radius, the positive max. pulse pressure (double pulse) was 31 MPa with a pulse duration of 1.5 μs. The cylinder axis was perpendicular to the wave-propagation direction.

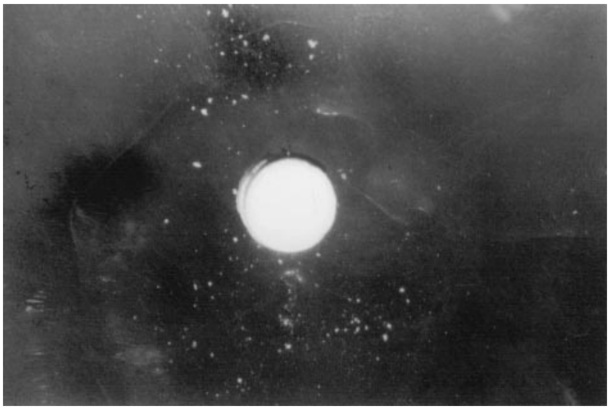

Fig. 10. First cleavage of a cylindrical stone as in Fig. 8, but with the cylinder axis parallel to the wave-propagation direction. The cleavage is now perpendicular to the wave-propagation direction.

higher fragility of the stone, we observed up to five first cleavage planes parallel to the wave vector. Three cleavage planes parallel to the wave vector have been observed also in earlier experiments (Dahake and Gracewski 1997b). Obviously, the increase of the number of first cleavage planes with pulse pressure and fragility is a consequence of the cooperative interaction of microcracks with coalescence to more than one fissure, as will be discussed in the theoretical section.

Small fragments

The development of fragmentation under a pulse pressure $p_+ = 25$ MPa, the pulse width of 1.0 μs and the -6-dB focal diameter of 22 mm for 4 individual artificial stones of 15 mm diameter with increasing pulse number is shown in Fig. 13. The result indicates the increasing number of smaller fragments with fairly narrow fragment size distribution. This is in accord with a fragmentation mainly into two parts that we could observe also visually by looking at single fragments. For the final fragmentation in particles of 2-mm size, the stone was supported by the nylon grid with 2-mm mesh size, shown in Fig. 3. The observation of the cleavage of natural and artificial stones under moderate pulse pressure into two fragments and, further, the visual evidence that smaller stones and fragments after a finite pulse number also split into two parts indicates that ESWL with a large focus can be described in terms of "binary fragmentation" (F. Kun, personal communication, 1999) (Redner 1990). Despite the fact that this has to be checked by careful measure-

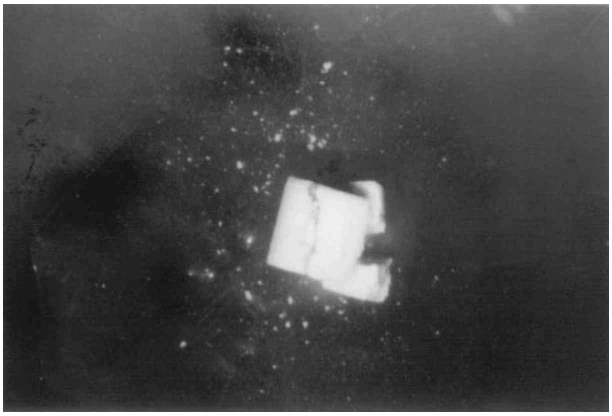

Fig. 9. Further cleavage of the cylindrical stone in Fig. 8 into planes parallel and perpendicular to the wave-propagation direction.

Fig. 11. First cleavage of a larger cylindrical artificial stone (HMT) into several fissures parallel and perpendicular to the wave-propagation direction. The stone dimensions were 10 × 10 mm.The positive pulse pressure was 31 MPa.The cylinder axis was perpendicular to the wave-propagation direction.

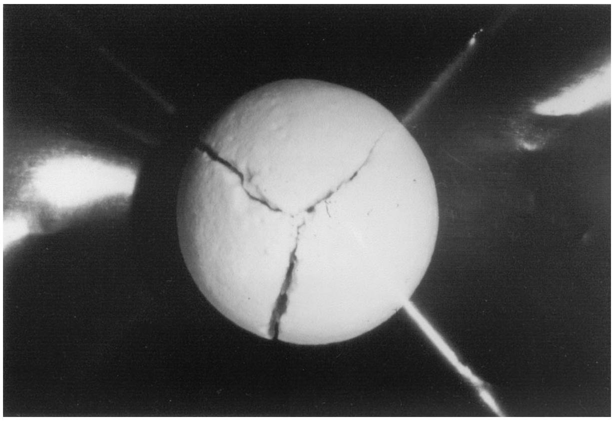

Fig. 12. First cleavage of a spherical stone (HMT 15 mm diameter) into three first cleavage surfaces at increased pulse pressure of 37 MPa. The wave-propagation direction was perpendicular to the picture plane.

ments of the fragment size distribution (Redner 1990), in progressive fragmentation under controlled experimental conditions or by computer simulations, the following simple experimental test and analysis might give a more direct answer.

The fragmentation ratio

Because the number of pulses needed for the fragmentation to 2-mm particle size is expected to be related to the number of pulses for the first cleavage, the corresponding "fragmentation ratio" has been determined experimentally for spherical stones. Figure 14 shows the

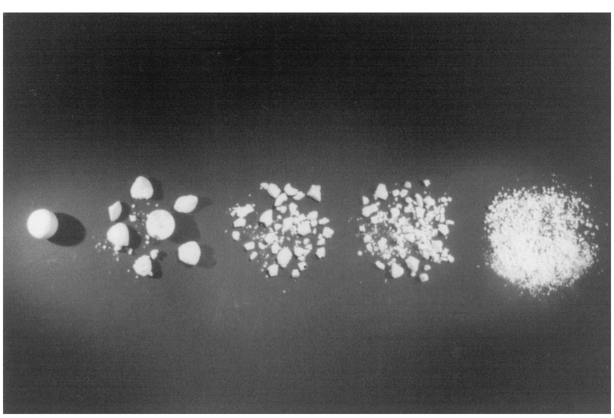

Fig. 13. Fragmentation results for artificial stones (HMT 15 mm diameter) with increasing number of shock waves. The pulse pressure was 25 MPa, with 1-μs pulse duration and a -6-dB focal diameter of 22 mm. The figure shows, from left to right, first the stone, then fragmentation after 7 pulses, 60 pulses, 120 pulses and 500 pulses, with particle size below 2 mm. The results were obtained using a separate stone for each fragmentation.

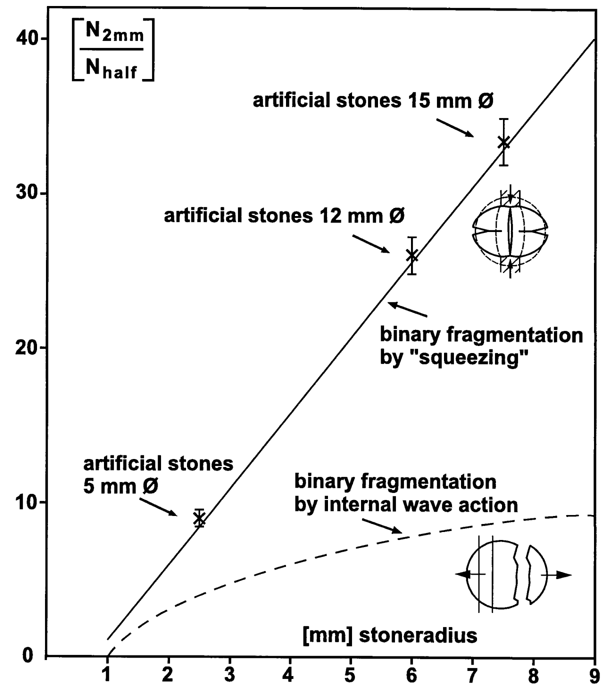

Fig. 14. Ratio of the number of pulses needed for 2-mm size fragmentation and of the number needed for the first cleavage. The experimental data are averages of 12 stones of 5-mm diameter, 10 stones of 12-mm diameter and 7 stones of 15-mm diameter taken at a pulse pressure of 11 MPa, pulse duration of 1.8 μs and -6-dB focal width of 18 mm. The error bars correspond to the SEM. The agreement with the theoretical result eqn (16) (full line), which depends only on the sphere radius without any fitting parameter as predicted by the quasistatic "squeezing" model of binary fragmentation, does not indicate significant contributions by cavitation or binary fragmentation by wave propagation and reflection inside the stone. The corresponding theoretical dependence eqn (11) of the latter mechanism on the stone radius has been introduced for comparision as a dotted line.

experimental data obtained with artificial stones from different sources with diameters of 5 mm (12 HMT stones), 12 mm (10 Dornier stones) and 15 mm (7 HMT stones) measured with pressure pulses of 11 MPa peak pressure, 1.8 μs pulse duration and 18 mm -6 dB focus diameter in comparison with the prediction of our theoretical model (full line) as derived in the next section. The error bars correspond to the standard error of the mean of the measurements.

Evidently, the good agreement between experiment and our theoretical model confirms the visual observation of the squeezing mechanism together with binary fragmentation. For comparison, the dotted line in Fig. 14 shows the expected result for binary fragmentation instead by "wave propagation inside the stone" as also discussed in the theoretical section. From these results, it is evident that stone fragmentation by wave propagation and reflection inside the stone, as well as cavitation, under our experimental conditions do not contribute significantly to fragmentation. It has to be determined whether or not with changed shock-wave parameters, such as higher pulse pressures, increased negative pressure, sharper focusing, etc., deviations from the binary squeezing model indicate significant other fragmentation contributions.

THEORY OF QUASISTATIC BINARY FRAGMENTATION

Fragmentation of brittle composite materials in general

Kidney stones, gallstones, etc. are viewed as composite brittle materials with some kind of cement, and artificial stones are modeled accordingly. They exhibit, under constantly increased load, a breaking threshold that is higher for compression than for dilatation. The maximum compression and tensile stress for wetted stones range from 1 to 2 MPa and 0.5 to 1 MPa, respectively (Delius 1994; Zhong and Preminger 1994). These values are well below the present clinical ESWL pressures, ranging from about 30 MPa to 100 MPa.

The breaking or cleaving process, in principle, can be described by the nucleation, growth and coalescence (Lokhandwalla and Sturtevant 2000; Sturtevant and Lokhandwalla 1998) of microflaws or microcracks under the repeated action of dilatation strain until a complete crack or fragmentation interface is generated. In the literature, shear deformation as cause for fracture is mentioned, in addition. In crystalline materials, this primarily causes dislocation movement but, under strong loading conditions, breaking can also be described because shear is also represented by orthogonal compression and dilatation rotated by 45° with respect to the shearing direction.

Preexisting microflaws in composite brittle materials, such as kidney stones or artificial stones, are the nuclei for the growth of microcracks (Camacho and Ortiz 1966) under strain. For strong loads much higher than the breaking threshold, the microcracks can grow independently, resulting in a “one pulse shattering” destruction into a multitude of fragments. By repeated application of weaker pressure or strain pulses just above the breaking threshold, microcracks will also grow but, after a finite number of pulses, coalesce to a large fissure (Fig. 15) that results into breaking of the object into two parts with the corresponding cleavage interfaces. In this situation of fatigue, the coalescence of the growing microcracks is caused by the mechanical interaction and stronger growth of microcracks in one single plane perpendicular to the strain direction. Of course, with increased fragmentation strength, also more than one first cleavage plane can be explained in a corresponding way. This

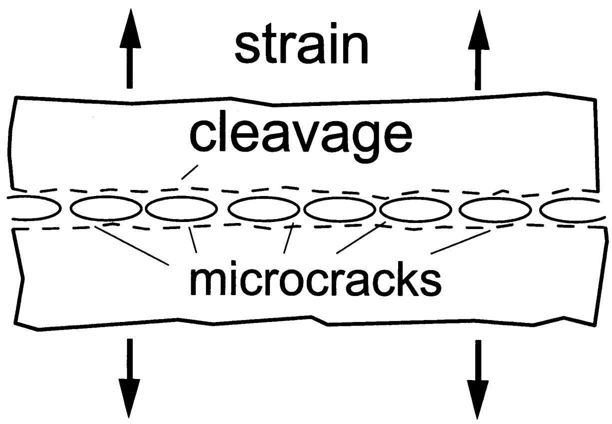

Fig. 15. Schematic view of the growth of microcracks under repeated strain pulses and their final coalescence to a macroscopic fissure.

general mechanism has been analysed in the framework of a “cohesive zone model” (Camacho and Ortiz 1966).

Quantitative fragmentation models

Recently, the fragmentation process in ESWL has been treated in terms of a dynamic fracture or fatigue process (Lokhandwalla and Sturtevant 2000; Sturtevant and Lokhandwalla 1998) by the nucleation and growth of preexisting flaws or microcracks that grow and coalesce under repeated strain application until cleavage. The 1-D treatment uses the ideal situation of strain in one direction and gives an estimate of 2 to 10 repeated stress pulses for the cleavage into two fragments under realistic conditions. The number of pulses needed for cleavage scales with the reciprocal pulse duration, but the calculation does not predict a relation to the reciprocal pulse energy or to the square of the peak pressure as observed in most experiments. Because this treatment of fragmentation is based on the strain amplitudes and their critical values for fragmentation, a more general treatment of this problem using the energy theorem originally proposed by Griffith (1920) will be presented here. According to Griffith, the elastic energy stored in the volume of the elastic body immediately before fragmentation is, during breakage, completely converted to vibration, heat, surface-energy, molecular potential and other forms of energy that can be all attributed to the freshly generated fragmentation area. This theorem can be directly applied to the squeezing mechanism in ESWL.

The positive part of the pressure pulse acts on the stone or the fragments by quasistatic squeezing, as inferred from the observed cleavage orientations. Assuming, in addition, that the inhomogeneous strain distribution (Fig. 6) inside the stone and also in the fragments does not significantly change until the lower limit of the clinical accepted size of 2 mm is reached, the quasistatic elastic squeezing energy E_{el} in the stone (Morse and Ingard 1968) can be described by:

$$E_{el} = \frac{p^2}{2} \kappa V \alpha, \tag{1}$$

where p = positive (or also negative) peak pulse pressure, κ = compressibility, V = volume, and α = form-factor accounting for the inhomogeneous pressure distribution within V. Because the elastic energy within the stone available for the growth of cracks E_{elp} depends on the pulse duration t, this results in:

$$E_{elp} = \frac{p^2}{2} \kappa V \alpha \frac{t}{t_{cr}}, \tag{2}$$

with t_{cr} the characteristic time (Camacho and Ortiz 1966) for the coalescence of microcracks under stationary conditions. This time is expected to be the same for all fragments of the stone because it depends only on the distance of the initial microcracks and the speed of crack growth, which is also expected to be constant if the peak pressure does not change. The proportionality with time is in agreement with Lokhandwalla and Sturtevant (2000), further with " Miner's rule" (Miner 1945), and with the experimental experience that the fragmentation rate scales with the total available elastic energy. (It is to be mentioned here that a detailed accurate treatment of E_{elp} requires a more refined theory, by taking the proper volume and time integrals of the quasistatic elastic energy distributions in the stone generated by the spatial inhomogeneous and time-dependent wave pressure field at the stone surface.)

Finally, the total available elastic energy required for the first fragmentation into two parts is E_{elpn}, given by:

$$E_{elpn} = \frac{p^2}{2} \kappa V \alpha \frac{t}{t_{cr}} n(r), \tag{3}$$

with $n(r)$ = the number of pulses to fragment a spherical stone with radius r. In the fragmentation process, this energy is lost and converted to the surface generation energy E_{fr} of the fragment according to the theorem of Griffith (1920). With $E_{fr} = A \cdot \gamma$, A = fracture area, γ = specific surface generation energy, and with $E_{elpn} = E_{fr}$, according to the Griffith theorem, we arrive at the condition:

$$\frac{p^2}{2} \kappa V \alpha \frac{t}{t_{cr}} n(r) = A \cdot \gamma \tag{4}$$

using spherical approximation with:

$$V = \frac{4\pi}{3} r^3 \tag{5}$$

and $A = \pi r^2$. This leads to:

$$n(r) = \frac{3}{2} \cdot \frac{1}{r} \cdot \frac{t_{cr}}{t} \cdot \frac{1}{p^2} \cdot \frac{\gamma}{\kappa \cdot \alpha} \tag{6}$$

(*i.e.*, the number of pulses required to split a stone of radius r scales with $1/r$ and with the reciprocal elastic energy during the pulse). The $1/r$ dependence is well known in fragmentation (Redner 1990) as a general experience and expectation because smaller objects are more difficult to break.

Because, after the first fragmentation step, the fragments on the average have half the original volume, the most simple approximation is to treat these fragments again as spheres now with reduced radius r_1 and determine the number of pulses $n(r_1)$ needed for splitting again into two fragments.

Thus, starting with

$$V_0 = \frac{4\pi}{3} r_0^{\,3} \tag{7}$$

and

$$V_1 = \frac{1}{2} V_0 \tag{8}$$

we use

$$V_m = \frac{V_0}{2^m} \tag{9}$$

thus, arriving at

$$r_m = r_0 \cdot 2^{-\frac{m}{3}} \tag{10}$$

or

$$m = 3 \frac{\ln \frac{r_0}{r_m}}{\ln 2} \tag{11}$$

with m = the number of steps for binary fragmentation to end up with fragments of radius r_m, which can pass a sieve with mesh width of $2r_m$.

The total number of pulses S_{tot} needed to fragment the stone to the radius r_m is now given by the sum of the geometrical series:

$$S(m) = \sum_{k=0}^{k=m} n(r_k) \quad (12)$$

with:

$$n(r_k) = n(r_0) \cdot \frac{r_0}{r_k} \quad (13)$$

and

$$r_k = r_0 \cdot 2^{-\frac{k}{3}} \quad (14)$$

The sum formula of the geometrical series results in:

$$S(m) = n(r_0)\,\frac{(2^{\frac{1}{3}})^{m+1} - 1}{2^{\frac{1}{3}} - 1} \quad (15)$$

and, with eqn (11), we finally obtain the fragmentation ratio:

$$\frac{S(m)}{n(r_0)} = \frac{S\left(\frac{r_0}{r_m}\right)}{n(r_0)} = \frac{2^{\frac{1}{3}} \cdot \frac{r_0}{r_m} - 1}{2^{\frac{1}{3}} - 1} \quad (16)$$

Thus, the squeezing model together with binary fragmentation results in a linear dependence of the fragmentation ratio (*i.e.*, the ratio of the number of pulses *S(m)* needed for fragmentation to the final size of r_m) and the pulse number $n(r_o)$ for the first fragmentation.With the mesh size of 2 mm, the radius r_m and r_0 enter in mm as radius of the fragments and the model stone, respectively. In this way, the theoretical result eqn (16) as the full line in Fig. 14 for fragmentation to 2-mm mesh size or 1-mm final radius has been introduced. It is to be emphasized that the fragmentation ratio eqn (16) depends only on the stone radius and the final fragment size. Different stone fragility or the pulse pressure amplitude, for example, do not enter. Figure 14 also shows by a dotted line the theoretical prediction for binary fragmentation by wave propagation and sound soft reflection within the stone. In this case, the energy available for fragmentation scales with the cross-section of the stone and not with the volume. Therefore, the pulse number for fragmentation does not depend on the radius. Consequently, the fragmentation ratio is given directly by eqn (11) using the number *m* of binary fragmentation steps that scale logarithmically with the ratio of the stone-to-fragment radius.

DISCUSSION

Apparently, the observation of cleavage planes parallel and perpendicular to the wave propagation direction is in accord with the model of quasistatic circumferential squeezing. In addition the “fragmentation ratio” (*i.e.*, the ratio of the pulse number for fragmentation to 2 mm size to the pulse number for the first cleavage) is in agreement with a simple quantitative evaluation of this model in terms of binary fragmentation, which is also directly observed in the experiments. Surprisingly, Fig. 14 does not show a significant contribution of fragmentation by wave propagation and reflection inside the stone. Possibly, this can be explained by the fact that in the “slower” squeezing mechanism there is sufficient time (Freund 1998) for the mechanical interaction between microcracks during coalescence. This time might be not available in the “faster” wave propagation inside the stone. Anyway, the direct evidence for the squeezing mechanism is the observation of cleavage planes parallel and perpendicular to the wave-propagation direction.

So far, the direct contribution of the negative pressure wave that follows the positive pressure peak has not been discussed in detail, but it is expected that there is a significant contribution to the growth of microcracks already generated by the squeezing mechanism. Therefore, the cleavage directions of squeezing are not changed as well as the theoretical result of the model.

The contribution of the negative pressure with $p_- = -3.5$ MPa to fragmentation by cavitation in our experiments (*cf*. Fig. 14), does not appear to be of significant influence. With higher negative pressures, the first erosion of the anterior and posterior surface of artificial stones evidently is caused by cavitation. Therefore, the cavitation craters in this case may also nucleate microflaws for the growth of cleavage planes parallel to the wave-propagation direction. Nevertheless, it would be difficult to explain the agreement between experiment and theory of binary fragmentation in the squeezing model by cavitation. Cavitation erosion, on the other hand, will become very important if the squeezing mechanism is suppressed by static prestress, as in the case of larger urether stones. In this situation, the microcracks cannot grow under repeated pulse exposure because they tend to be closed again after each pressure pulse. This is a similar situation as in prestressed concrete or ceramics with a significant increase of breaking strength. It has been observed (Parr et al. 1992) that stones enclosed in a latex or silicone rubber hose as model for urether stones are mainly eroded by cavitation at the lower and upper surfaces not in contact with the hose. In this situation, the number of pulses needed for fragmentation can be one order of magnitude larger than for a free stone.

Cavitation evidently is also very important for opening up the cleavage planes (Sass et al. 1991) and the motion of fragments by the direct impact of the liquid of the collapsing bubbles or of jets (Crum 1988) generated by cavitation bubble collapse close to the fragment surfaces. It has been also observed (Sass et al. 1991) that cavitation takes place in cleavage planes after or during cleavage because kidney stones and artificial stones are completely wetted, with liquid filling all cracks and microcracks. This is supported by the fact that the static breaking strength is reduced by more than a factor of two for wetted artificial stones as compared to dry stones. Evidently, the water penetrates into the crack tips, thereby reducing the interface energy and the surface potential. This is also well known from cutting glass with a diamond knife, where water reduces the breaking strength significantly.

Thus, the growth of cracks under pulse exposure is automatically generating cavitation nuclei in the liquid filled crack tip. This, in fact, is a new mechanism of "dynamic" cavitation nucleation.

Because many lithotripters of the third generation use sharp focusing from 2 mm to 6 mm −6 dB focus diameter, the fragmentation efficiency is measured by the volume or weight of material (Dreyer et al. 1998; Granz and Köhler 1992; Vakil et al. 1991) eroded for a finite number of pulses. A theoretical treatment of this situation is more difficult because the size of the generated particles is less defined compared to sieving with 2 mm mesh size.

If, on the other hand, under realistic conditions the fragment size gets close to the focus diameter, the squeezing model will finally dominate fragmentation.

Obviously, the mechanism of squeezing suggests for high stone fragmentation efficiency in ESWL, focal diameters up to 20 mm with pulse duration up to 2 μs, but not necessarily a sharp shock front. In water and tissue, this corresponds to a −6-dB compression zone of 3 mm width still short enough to result in fragments of 2 mm size. The focal positive pressure peak can be reduced to the lower pressure range of 10 MPa to 30 MPa because this is completely sufficient to overcome the breaking threshold (Delius 1994; Zhong and Preminger 1994) of max. 2 MPa for known concrements and artificial stones. It should be noted that the artificial stones of 15 mm diameter in our experiments with 18 mm −6-dB focal width and 1.8 μs pulse duration could be fragmented to 2 mm particle size with 900 pulses of 11 MPa, 200 pulses of 25 MPa and 130 pulses of 35 MPa. This is to be compared with other *in vitro* fragmentation results (Köhrmann et al. 1993).

Negative pressures causing cavitation and, possibly, side effects can be reduced to −3.5 MPa. Coupling the pressure pulse or shock wave into the patient by use of a water-filled rubber cushion will prevent cavitation at the skin if the coupling jelly is free of bubbles. Cavitation nucleation in the bubble-free jelly does not lead to the growth of cavitation bubbles as a consequence of the high viscosity of the jelly. On the other hand, bubbles already present in the jelly at the skin will collapse vehemently under the positive pressure pulse and produce pain. The results of clinical ESWL studies (Du and Eisenmenger 1999) of the treatment of kidney stones under the conditions of increased focal area, larger pulse width and reduced positive and negative pressure are awaited. In addition to the more uniform pressure exposure of the distributed fragments, further possible advantages of a larger focal width are reduced aperture and increased positional flexibility, ease of treating larger stones with wider fragment distribution in space and avoiding the necessity of x-ray control during treatment because ultrasonic positioning appears as sufficient. This requires comparative clinical studies (Renner and Rassweiler 1999) according to the present standards.

CONCLUSION

"Squeezing" appears to be the dominant fragmentation mechanism in ESWL. This might open up possibilities to further increase the stone destruction efficiency with minimised side effects by using focus diameters up to 20 mm, a pulse width of up to 2 μs and reduced pulse pressures in the range from 10 MPa to 30 MPa. Investigations of the detailed pressure field characteristics in relation to the fragmentation efficiency field *in vitro* and in comparison with corresponding clinical studies are necessary.

Acknowledgements—The author is especially grateful to M. Delius for a multitude of informative and fruitful discussions about the questions of stone destruction, also providing me with the wide body of ESWL literature and supporting my interest and activities in this field over years. The author is also very grateful to F. Eisenberger and J. Rassweiler for the enthusiastic support of my work and numerous advice and help. The author extends special thanks to F. Ueberle for many stimulating discussions and for supporting and promoting the need for precise measurement methods in ESWL, and thanks N. Brill for generously supplying HMT artificial stones of different size. The author expresses gratitude to H. Herrmann and F. Kun from the Institute of Computer-physics of the University of Stuttgart for introduction into the literature of fragmentation physics and information about the importance of the process of binary fragmentation. The author is very grateful to F. Brümmer, D. F. Hülser, U. Irmer and D. Suhr from the Biologic Institute of our University for their great help and for many fruitful and enthusiastic discussions, and is especially indebted to D. F. Hülser and U. Irmer for critically reading the manuscript and their valuable suggestions. The author thanks B.Gompf, M. Köhler, B. Küssner, K. Laβmann, R. Pecha, J. Staudenraus, Z. Q. Wang and W. Wölfel, from the Physical Institute of the University of Stuttgart, for their important work, suggestions, help and stimulating discussions in the shock-wave field, and is especially grateful to R. Heckhorn and E. Wagner for their skill and technical competence in building the experimental systems. Last, but not least, the author is especially indebted to

X. X. Du for the successful cooperation in clinical studies in the P.R. of China.

REFERENCES

Brümmer F, Staudenraus J, Eisenmenger W, Hülser DF. Fundaments of the physics and medical and biological effects of differently generated shockwaves with respect to the clinical application. BMFT 1992;8706:6.

Camacho GT, Ortiz M. Computational modelling of impact damage in brittle materials. Int J Solids Structures 1966;20:2899–2938.

Chaussy C, Eisenberger F, Jocham D, Wilbert D. High energy shock waves in medicine. Stuttgart, New York: Thieme, 1997.

Coleman AJ, Saunders JE. A review of the physical properties and biological effects of the high amplitude acoustic field used in extracorporeal lithotripsy. Ultrasonics 1993;31:75–89.

Crum LA. Cavitation microjets as a contributory mechanism for renal calculi disintegration in ESWL. J Urol 1988;140:1587.

Dahake G, Gracewski SM. Finite difference predictions of P-SV wave propagation inside submerged solids. I. Liquid-solid interface conditions. J Acoust Soc Am 1997a;102:2125–2137.

Dahake G, Gracewski SM. Finite difference predictions of P-SV wave propagation inside submerged solids. II. Effect of geometrie. J Acoust Soc Am 1997b;102:2138–2145.

Delius M. Medical applications and bioeffects of extracorporeal shock waves. Shock Waves 1994;4:55–72.

Delius M. Minimal static excess pressure minimises the effect of extracorporeal shock waves on cells and reduces it on gallstones. Ultrasound Med Biol 1997;23:611–617.

Delius M. History of shock wave lithotripsy. Proceedings of the 15th International Symposium on Nonlinear Acoustics 2000:23–32.

Delius M, Gambihler S. Effect of shock waves on gallstones and materials. In: Paumgartner G, Ferrucci J, Burhenne J, eds. Lithotripsy and related techniques for gallstone treatment. Proceedings of the 3rd International Symposium on Biliary Lithotripsy. St. Louis: Mosby Year Book, 1991:27–33.

Dreyer T, Riedlinger RE, Steiger E. Experiments on the relation of shock wave parameters to stone disintegration. 135th ASA Conference Proceedings 1998:2811–2812.

Du XX, Eisenmenger W. Clinical ESWL study with a selffocussing electromagnetic generator and large focus. Stuttgart: Wuxian, 1999.

Eisenberger F, Miller K, Rassweiler J. Stone therapy in urology. Stuttgart, New York: Thieme, 1991.

Eisenmenger W. Einrichtung zur berührungsfreien Zertrümmerung von Konkrementen im Körper von Lebewesen - Selbstfokussierender elektromagnetischer Stoβwellengenerator. Deutsche Patentschrift DE 3312014 C2 v. 2. 4. 1983

Eisenmenger W. Physikalisch-medizinische Aspekte selbstfokussierter elektromagnetisch erzeugter Stoβwellen. Verh Ber Dtsch Ges Urol 1988;39:69–70.

Eisenmenger W. Shock wave measuring techniques in liquids. 135th ASA Conference Proceedings 1998:2793–2794.

Freund LB. Dynamic fracture mechanics. Cambridge, UK: Cambridge University Press, 1998.

Granz B, Köhler G. What makes a shockwave efficient in lithotripsy? J Stone Dis 1992;4:123–128.

Griffith AA. The phenomenon of rupture and flow in solids. Philo Trans Roy Soc (London) 1920;A221:163–198.

Heimbach D, Munver R, Zhong P, Jacobs J, Hesse A, Müller SC, Preminger GM. Acoustic and mechanical properties of artificial stones in comparison to natural kidney stones. J Urol 2000;164: 537–544.

Holtum D. Eigenschaften und Desintegration von menschlichen Gallensteinen unter Stoβwellenwirkung. Ph.D. Thesis, Stuttgart: University of Stuttgart, 1993.

IEC. Ultrasonics—pressure pulse lithotripters—characteristics of fields Report 61846. Geneva, Switzerland: IEC, 1998.

Irmer U. Wirkung hochenergetischer Schallwellen auf Hybrid-Multizell-Sphäroide. Ph.D. Thesis. Stuttgart: University of Stuttgart, 1997.

Irmer U, Brümmer F, Staudenraus J, Hülser DF, Eisenmenger W. Artificial stone fragmentation measurements with selffocusing electromagnetic shockwave generators. 2001, (in press).

Koch H, Grünewald M. Disintegration mechanism of weak acoustic shock waves. Ultrasound Int Conf Proc 1989:1136–1141.

Köhrmann KU, Kahmann FU, Weber M, Rassweiler J, Alken P. Vergleich verschiedener Lithotripter anhand der Desintegrativen Effektivität (DE) und Desintegrativen Bandbreite (DB) am in-vitro-Steinmodell. Akt Urol 1993;24:320–325.

Lokhandwalla M, Sturtevant B. Fracture mechanics model of stone comminution in ESWL and implications for tissue damage. Phys Med Biol 2000;45:1923–1949.

Miner MA. Cumulative damage in fatigue. J Appl Mech 1945:A159–A164.

Morse PM, Ingard KU. Theoretical acoustics. New York: McGraw. Hill, 1968:233.

Müller M. Dornier Lithotripter im Vergleich - Vermessung der Stoβwellenfelder und Fragmentationswirkungen. Biomed Technik 1990;35:250–262.

Parr NJ, Pye SD, Ritchie AWS, Tolley DA. Mechanisms responsible for diminished fragmentation of ureteral calculi: An experimental and clinical study. J Urol 1992;184:1079–1083.

Redner S. Fragmentation. In: Herrmann HJ, Roux S, eds. Statistical models for the fracture of disordered media. North Holland: Elsevier Science B.V., 1990:321.

Renner C, Rassweiler J. Treatment of renal stones by extracorporal shock wave lithotripsy. Nephron 1999;81:71–81.

Sass W, Bräunlich M, Dreyer HP, Matura E, Folberth W, Priesmeyer HG, Seifert J. The mechanisms of stone disintegration by shock waves. Ultrasound Med Biol 1991;17:239–243.

Staudenraus J. Erzeugung und Ausbreitung freifeldfokussierter Hochenergiedruckimpulse in Wasser. Ph.D. Thesis. Stuttgart: University of Stuttgart, 1991.

Staudenraus J, Eisenmenger W. Fibre-optic probe hydrophone for ultrasonic and shock-wave measurements in water. Ultrasonics 1993;31:267–273.

Steiger E. Modellierung der Ausbreitung in extrakorporalen Therapien eingesetzter Ultraschallimpulse hoher Intensität. Karlsruhe: Institut für Höchstfrequenztechnik und Elektronik der Universität Karlsruhe, 1998.

Steiger E, Marlinghaus EH. Modeling the Storz Modulith SL 10 shock wave lithotripter. World Congress on Ultrasonics, Yokohama, 1997:490–491.

Sturtevant B, Lokhandwalla L. Biomechanical effects of ESWL shock waves. 135th ASA Conference Proceedings. 1998:2493–2494.

Ueberle F. Acoustic parameters of pressure pulse sources used in lithotripsy and pain therapy. In: Chaussy Ch, ed. High energy shock waves in medicine. Stuttgart, New York: Thieme, 1997:76–85

Ueberle F. Pressure pulses in medicine. Shock focussing effects in medical science and sonoluminescence. In: Srivastava RC, Leufloff D, Takayama K, Groenig H, eds. Heidelberg: Springer-Verlag, (in press).

Vakil N, Gracewski SM, Everbach EC. Relationship of model stone properties to fragmentation. J Lithotripsy Stone Dis 1991;3:304–310.

Wang ZQ, Lauxmann P, Wurster C, Köhler M, Gompf B, Eisenmenger W. Impulse response of a fiber optic probe hydrophone determined with shock waves in water. J Appl Phys 1999;85:2514–2516.

Xi X, Zhong P. Improvement of stone fragmentation during shock-wave lithotripsy using a combined EH/PEAA shock-wave generator—in vitro experiments. Ultrasound Med Biol 2000;26:457–467.

Zhong P, Preminger GM. Mechanisms of differing stone fragility in extracorporal shockwave lithotripsy. J Endourol 1994;8:263–268.